RSC Advances

PAPER

Cite this: *RSC Adv.*, 2017, **7**, 13444

Observation of up-conversion luminescence polarization control in Sm^{3+}-doped glass under an intermediate femtosecond laser field

Ye Zheng,[a] Wenjing Cheng,*[b] Yunhua Yao,[a] Cheng Xu,[c] Donghai Feng,[a] Tianqing Jia,[a] Jianrong Qiu,[c] Zhenrong Sun[a] and Shian Zhang*[ad]

The polarization modulation strategy of the femtosecond laser field was shown to be a well-established method to control up-conversion luminescence in rare-earth ions. In this work, we further extend the polarization control behavior from weak to intermediate femtosecond laser fields. We experimentally show that the polarization control efficiency of the up-conversion luminescence in the Sm^{3+}-doped glass will be affected by the femtosecond laser intensity, which decreases with the increase of the laser intensity. We theoretically propose a fourth-order perturbation theory to explain the experimental observation, which includes the two-photon and four-photon absorptions, and the destructive interference between the two-photon and four-photon absorption will result in the suppression of the polarization control efficiency due to their different polarization control degrees. These experimental and theoretical results provide a new insight into understanding the polarization control process of up-conversion luminescence in rare-earth ion doped luminescent materials under an intermediate femtosecond laser field, and also can open a new opportunity for the polarization control application in some related areas.

Received 14th December 2016
Accepted 21st February 2017

DOI: 10.1039/c6ra28194j

rsc.li/rsc-advances

1. Introduction

The up-conversion luminescence of rare-earth ions by converting low frequency photons to high frequency emissions *via* two-photon or multi-photon absorption has attracted great attention for its excellent optical properties, such as photo-stability, narrow spectrum, near infrared excitation, large Stokes shift, long luminescence lifetime, and well-defined emission bands.[1,2] In practical applications, the up-conversion luminescence of rare-earth ions has been widely applied in laser sources,[3,4] fiber-optic communication,[5,6] light-emitting diodes,[7] solar cells,[8] color displays,[9,10] biolabeling and biomedical sensing,[11–14] and so on. In order to further extend the various related application areas, it is very important to control the up-conversion luminescence of rare-earth ions in real-time, dynamical and reversible manners. Recently, several schemes have been proposed to realize the control manner, such as electric field,[15] magnetic field,[16] Plasmon,[17] temperature,[18] laser wavelength,[19] laser pulse duration,[20] laser repetition,[21] and so on. We proposed a femtosecond pulse shaping technique by the spectral phase modulation to tune or control the up-conversion luminescence of rare-earth ions.[22,23] For example, the up-conversion luminescence intensity in Er^{3+}-doped glass sample can be effectively suppressed by a π phase step modulation.[22] The green and red up-conversion luminescence in Er^{3+}-doped $NaYF_4$ nanocrystals can be tuned by a square phase modulation.[23] Moreover, we also showed that the femtosecond laser polarization technique is a feasible method to control the up-conversion luminescence in the rare-earth ions.[24,25] For example, the up-conversion fluorescence intensity of Dy^{3+}-doped glass sample can be controlled by both the laser polarization and phase modulations, and the laser polarization will affect the control efficiency of the laser phase modulation.[24]

The laser polarization strategy has shown to be a well-established tool in the control of the up-conversion luminescence in rare-earth ions.[24,25] However, these previous studies mainly focused on the laser polarization control under the weak femtosecond laser field. In this work, we further extend this polarization control behavior to the intermediate femtosecond laser field. We experimentally demonstrate that the femtosecond laser intensity will affect the polarization control efficiency of the up-conversion luminescence in the Sm^{3+}-doped glass sample, and the higher laser intensity will yield the lower polarization control efficiency. We theoretically show that the higher order nonlinear optical effect (*i.e.*, four-photon

[a]*State Key Laboratory of Precision Spectroscopy, East China Normal University, Shanghai, 200062, People's Republic of China. E-mail: sazhang@phy.ecnu.edu.cn*

[b]*School of Physics and Electrical Information, Shangqiu Normal University, Shangqiu, 476000, People's Republic of China. E-mail: 0110wenjing@163.com*

[c]*State Key Laboratory of Silicon Materials, Zhejiang University, Hangzhou, 310027, People's Republic of China*

[d]*Collaborative Innovation Center of Extreme Optics, Shanxi University, Taiyuan, Shanxi 030006, People's Republic of China*

absorption) will occur under the higher femtosecond laser intensity, which can induce a destructive interference with the two-photon absorption, and finally results in the suppression of the polarization control efficiency due to their different polarization control degrees. The proposed theoretical model can well explain the experimental observation.

2. Experimental setup

In our experiment, the Sm^{3+}-doped glass sample is prepared with the composition of 40% SiO_2, 25% Al_2O_3, 18% Na_2CO_3, 10% YF_3, 7% NaF and 0.5% Sm (in mol%). The mixed raw materials are melted in a platinum crucible with lid, which are treated for 45 minutes at the temperature of 1450 °C in ambient atmosphere, and then molded in a brass mould followed by a 10 hour anneal at the temperature of 450 °C. Finally, the glass products are further processed through incision and polishing, and are used in our optical measurement. The schematic diagram of our experimental arrangement for the laser polarization control of up-conversion luminescence in the Sm^{3+}-doped glass is shown in Fig. 1. Here, a Ti:sapphire mode-locked femtosecond laser (Spitfire regenerative amplifier from Spectra-Physics Co.) is used as the excitation source with the pulse width of about 50 fs, the central wavelength of 800 nm and the repetition rate of 1 kHz, and an attenuator is used to vary the laser intensity, and a $\lambda/4$ plate is used to change the laser polarization. The polarization modulated femtosecond laser pulse is focused into the Sm^{3+}-doped glass sample with a lens of 50 mm focal length. Here, the diameter of the spot size at the sample is about 9.8 μm. All the up-conversion fluorescence signals radiated from the glass sample are collected perpendicularly and measured by a spectrometer with charge-coupled device (CCD).

3. Results and discussion

The UV-VIS-NIR absorption spectrum of the Sm^{3+}-doped glass sample is measured by a U-4100 spectrophotometer (Hitachi), and the experimental result is shown in Fig. 2(a). It can be seen that only one absorption band around the wavelength of 400 nm is observed, which is corresponding to the excited state $^6P_{3/2}$. Moreover, the up-conversion luminescence spectrum in the range of 300 to 800 nm under the 800 nm femtosecond laser

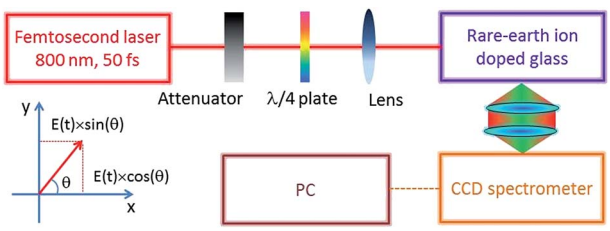

Fig. 1 The schematic diagram of the experiment arrangement for the polarization control of up-conversion luminescence in the Sm^{3+}-doped glass sample under the intermediate femtosecond laser field excitation. Here, an attenuator is used to vary the laser intensity, and a $\lambda/4$ plate is used to change the laser polarization.

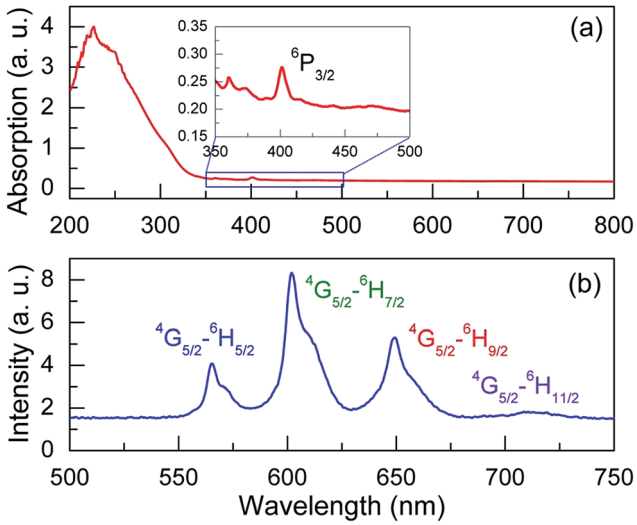

Fig. 2 The UV-VIS-NIR absorption spectrum of Sm^{3+}-doped glass sample (a), and the up-conversion luminescence spectrum in the visible light region under the 800 nm femtosecond laser pulse excitation with the laser intensity of 4.2×10^{13} W cm^{-2} (b).

pulse excitation with the laser intensity of 4.2×10^{13} W cm^{-2} is shown in Fig. 2(b). One can see that there are four up-conversion luminescence signals at the wavelengths of 565, 602, 649 and 709 nm, which can be attributed to the transition processes of $^4G_{5/2} \rightarrow {}^6H_{5/2}$, $^4G_{5/2} \rightarrow {}^6H_{7/2}$, $^4G_{5/2} \rightarrow {}^6H_{9/2}$, $^4G_{5/2} \rightarrow {}^6H_{11/2}$, respectively. The four up-conversion luminescence signals are all derived from the population of the excited state $^4G_{5/2}$, and therefore will have the same polarization control behavior. Here, we choose the up-conversion luminescence signal at the wavelength of 602 nm to analyze the polarization control behaviors under the different femtosecond laser intensities.

Fig. 3 shows the up-conversion fluorescence intensities by varying the quarter-wave ($\lambda/4$) plate angle θ with the

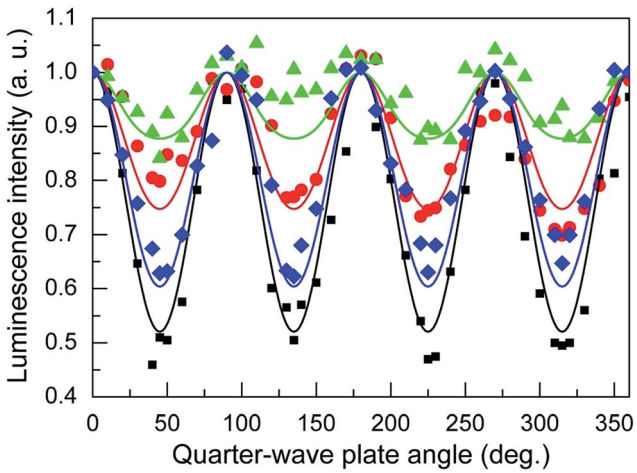

Fig. 3 The normalized up-conversion fluorescence intensity by varying the quarter-wave ($\lambda/4$) wave plate angle with the laser intensities of 2.1×10^{13} (black squares), 3.15×10^{13} (blue diamonds), 4.2×10^{13} (red circles) and 8.4×10^{13} W cm^{-2} (green triangles), together with the theoretical simulations (lines).

femtosecond laser intensities of 2.1×10^{13} (black squares), 3.15×10^{13} (blue diamonds), 4.2×10^{13} (red circles) and 8.4×10^{13} W cm^{-2} (green triangles), together with the theoretical simulations (lines). Here, all data are normalized by the corresponding transform-limited (TL) pulse excitation. As can be seen, by varying the quarter-wave ($\lambda/4$) plate angle (*i.e.*, the laser polarization), the up-conversion luminescence intensity can be suppressed but not be enhanced under both the lower and higher laser intensities, and is minimal value for the circular polarization. However, the polarization control efficiencies are different for the lower and higher laser intensities. It can be seen that the polarization control efficiency is nearly 50% in the lower laser intensity of 2.1×10^{13} W cm^{-2}, while decreases to 15% in the higher laser intensity of 8.4×10^{13} W cm^{-2}. Here, the control efficiency is defined by the function of $\eta = 1 - I^{min}/I^{max}$, where I^{min} and I^{max} are the minimal and maximal up-conversion luminescence intensities, respectively. That is to say, the laser intensity will affect the polarization control efficiency of the up-conversion luminescence in the Sm^{3+}-doped glass under the intermediate femtosecond laser field excitation, and the higher laser intensity will yield the lower polarization control efficiency.

In order to study the physical mechanism of the polarization control efficiency tuning by varying the femtosecond laser intensities, we propose a fourth-order perturbation theory model under the intermediate femtosecond laser field to explain above experimental observation, which includes the two-photon and four-photon absorptions. One simple method to verify the existence of four-photon absorption in our experiment is to measure the up-conversion luminescence by varying the femtosecond laser intensity, and the experimental results are shown in Fig. 4. As can be seen, the up-conversion luminescence intensity shows a slow increase and then fast increase behavior with the increase of the laser intensity, and therefore the experimental data in the lower and higher laser intensities can be linearly fitted by two solid lines with different slopes, respectively. It is obvious that the slope in the higher laser intensity is much larger than that in the lower laser intensity, which is due to the involvement of the four-photon absorption.

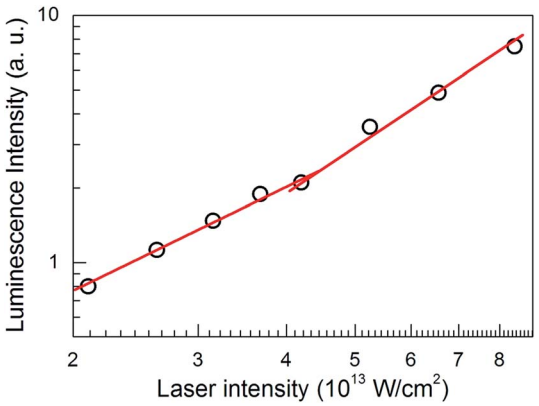

Fig. 4 The log–log plot of the up-conversion luminescence intensity by varying the femtosecond laser intensity with the linear polarization, together with the linear fitting.

In the lower laser intensity, the two-photon absorption dominates the whole excitation process, and therefore the slope is relatively low with about 1.8. However, in the higher laser intensity, the coexistence of two-photon and four-photon absorptions results in the slope increase with about 2.4.

Fig. 5 presents the energy level diagram of Sm^{3+} ion and the possible up-conversion excitation processes by the two-photon and four-photon absorptions. Here, the two states $^6H_{5/2}$ and $^6P_{3/2}$ represent the ground state |g> and final excited state |f>, respectively. It can be clearly seen that the two-photon absorption is a non-resonant excitation process, while the four-photon absorption is a resonance-mediated excitation process. In the two-photon absorption process, the initial population in the ground state |g> (*i.e.*, $^6H_{15/2}$) is pumped to the final excited state |f> (*i.e.*, $^6P_{3/2}$) by simultaneously absorbing two photons. However, the excitation pathway in the four-photon absorption process involves all the contributions of the non-resonant Raman parts *via* the virtual states |m> and |n>, where the four photons in the excitation process involves the three absorbed photons and one emitted photon. That is to say, the four-photon absorption in our study includes a stimulated downward process, which is different from the common four-photon absorption with the upward excitation during each step. In order to clearly describe the whole excitation process, the transition sequence of the two-photon or four-photon absorption is labeled by using the digital symbols of ①, ②, ③ and ④. The population in the final excited state $^6P_{3/2}$ can relax to the lower excited state $^4G_{5/2}$, and emits the up-conversion fluorescence signals by transition to the four states $^6H_{5/2}$, $^6H_{7/2}$, $^6H_{9/2}$ and $^6H_{11/2}$ (see Fig. 2(b)).

On the basis of above theoretical model, the transition amplitude A_f in the excited state $^6P_{3/2}$ under the intermediate femtosecond laser field excitation should involve the contributions from both the two-photon and four-photon absorptions, *i.e.*, $A_f^{(2)}$ and $A_f^{(4)}$. The second-order term $A_f^{(2)}$ (*i.e.*, non-resonant

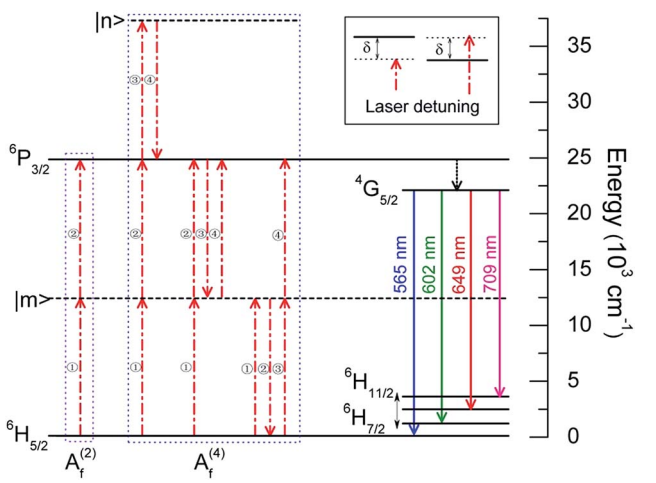

Fig. 5 The energy level diagram of Sm^{3+} ion and the possible up-conversion excitation processes for two-photon and four-photon absorptions, together with the laser detuning in the resonance-mediated four-photon absorption process.

two-photon absorption) includes all the non-resonant two-photon transition pathways, and can be described as[26]

$$A_f^{(2)} = \frac{i}{\hbar^2}|E_0|^2 A^{(2)}(\omega_{fg}), \quad (1)$$

with

$$A^{(2)}(\Omega) = \mu_{fg}{}^2 \int_{-\infty}^{\infty} \hat{E}(\omega)\hat{E}(\Omega-\omega)d\omega. \quad (2)$$

where ω_{fg} is the transition frequencies from the ground state |g> (*i.e.*, $^6H_{15/2}$) to the excited state |f> (*i.e.*, $^6P_{3/2}$), $\mu_{fg}{}^2$ is the corresponding dipole moment matrix elements. Here, we use the normalized spectral field $\hat{E}(\omega) = |E(\omega)|/|E_0|$ to represent the laser field shape, and E_0 is the maximal spectral amplitude. However, the fourth-order term $A_f^{(4)}$ (*i.e.*, resonance-mediated four-photon absorption) can be decomposed into the on-resonant and near-resonant parts. The on-resonant four-photon absorption is that the population in the ground state $^6H_{5/2}$ is firstly pumped to the excited state $^6P_{3/2}$ or ground state $^6H_{5/2}$ and then further pumped to the excited state $^6P_{3/2}$ by absorbing three photons and emitting one photon, and the near-resonant four-photon absorption is that the population in the ground state $^6H_{5/2}$ is directly pumped to the excited state $^6P_{3/2}$ without through the two states $^6P_{3/2}$ or $^6H_{5/2}$ with the three absorbed photons and one emitted photon. Thus, the four-order term $A_f^{(4)}$ can be approximated as[27–29]

$$A_f^{(4)} = A_f^{(4)\text{on-res}} + A_f^{(4)\text{near-res}}, \quad (3)$$

with

$$A_f^{(4)\text{on-res}} = \frac{i}{\hbar^4}|E_0|^4\left[i\pi\int_{-\infty}^{\infty} A_{abs}(\omega_{f(g)})A^{(2)}(\omega_{fg})A^{(R)}(0)d\omega_{f(g)}\right], \quad (4)$$

$$A_f^{(4)\text{near-res}} = \frac{i}{\hbar^4}|E_0|^4\left[-\wp\int_{-\infty}^{\infty} d\delta\frac{1}{\delta}A^{(2)}(\omega_{fg}-\delta)A^{(R)}(\delta)\right], \quad (5)$$

and $A^{(R)}(\delta)$ can be defined as

$$A^{(R)}(\delta) = \left(\mu_{gmg}{}^2 + \mu_{fmf}{}^2 + \mu_{fnf}{}^2\right)\int_{-\infty}^{\infty}\hat{E}(\omega+\delta)\hat{E}^*(\omega)d\omega, \quad (6)$$

where $\wp$ is the Cauchy principal value, $A_{abs}(\omega_{f(g)})$ represents the absorption line-shape function of the excited state |f> (*i.e.*, $^6P_{3/2}$) or ground state |g> (*i.e.*, $^6H_{15/2}$), δ is the laser detuning from the excited state |f> or ground state |i> (see inset of Fig. 5), and $\mu_{gmg}{}^2$, $\mu_{fmf}{}^2$, and $\mu_{fnf}{}^2$ are the effective non-resonant Raman coupling *via* the virtual state |m> or |n>. The on-resonant term $A_f^{(4)\text{on-res}}$ is excluded from the near-resonant term $A_f^{(4)\text{near-res}}$ by Cauchy's principal value operator $\wp$.

In the real experiment, the quarter-wave ($\lambda/4$) plate was usually used to change the laser polarization from line through elliptical to circular. Mathematically, the polarization modulated femtosecond laser field in the space can be decomposed into two orthogonal directions (*i.e.*, $\bar{e}_x$ and $\bar{e}_y$), and is written as[30]

$$E_{\lambda/4}(t) = \cos(\theta)E(t)\bar{e}_x + \sin(\theta)E(t)\bar{e}_y, \quad (7)$$

where θ is the angle between the input laser polarization direction and the $\lambda/4$ wave plate optical axis. It can be verified that the laser field is linear polarization for $\theta = m\pi/2$ (m = 0, 1, 2, …), circular polarization for $\theta = (2m+1)\pi/4$, and elliptical polarization for other angles θ. Fig. 6 shows the possible excitation pathways of non-resonant two-photon absorption process (a) and one of on-resonant four-photon absorption processes (b) by the polarization modulated femtosecond laser field. One can see that the two photons in the non-resonant two-photon absorption process can only come from the same polarization direction (*i.e.*, $\bar{e}_x\bar{e}_x$ and $\bar{e}_y\bar{e}_y$), while the four photons in the on-resonant four-photon absorption process can come from the different polarization directions (*i.e.*, $\bar{e}_x\bar{e}_x\bar{e}_y\bar{e}_y$ and $\bar{e}_y\bar{e}_y\bar{e}_x\bar{e}_x$) or the same polarization direction (*i.e.*, $\bar{e}_x\bar{e}_x\bar{e}_x\bar{e}_x$ and $\bar{e}_y\bar{e}_y\bar{e}_y\bar{e}_y$). Similar to the non-resonant two-photon absorption, the four photons in the near-resonant four-photon absorption process can only come from the same polarization direction (*i.e.*, $\bar{e}_x\bar{e}_x\bar{e}_x\bar{e}_x$ and $\bar{e}_y\bar{e}_y\bar{e}_y\bar{e}_y$). One can see that the polarization modulated femtosecond laser field can induce several different excitation pathways in the two-photon and four-photon absorption processes. Thus, the transition amplitudes in the excited state $^6P_{3/2}$ through these different excitation pathways can be written as

$$P_{xx} = \cos^2(\theta)A_f^{(2)} \quad (8)$$

$$P_{yy} = \sin^2(\theta)A_f^{(2)} \quad (9)$$

$$P_{xxxx} = \cos^4(\theta)A_f^{(4)\text{near-res}} + \cos^4(\theta)A_f^{(4)\text{on-res}}, \quad (10)$$

$$P_{yyyy} = \sin^4(\theta)A_f^{(4)\text{near-res}} + \sin^4(\theta)A_f^{(4)\text{on-res}}, \quad (11)$$

$$P_{yyxx} = \sin^2(\theta)\cos^2(\theta)A_f^{(4)\text{on-res}}, \quad (12)$$

$$P_{xxyy} = \cos^2(\theta)\sin^2(\theta)A_f^{(4)\text{on-res}}. \quad (13)$$

As can be seen, all these photons in eqn (8) and (10) come from the horizontal polarization direction (*i.e.*, $\bar{e}_x$), and therefore the two excitation pathways can occur the destructive or constructive interference. Similar behavior can be found in eqn (9) and (11), where all the photons come from the perpendicular polarization direction (*i.e.*, $\bar{e}_y$). Thus, the total transition

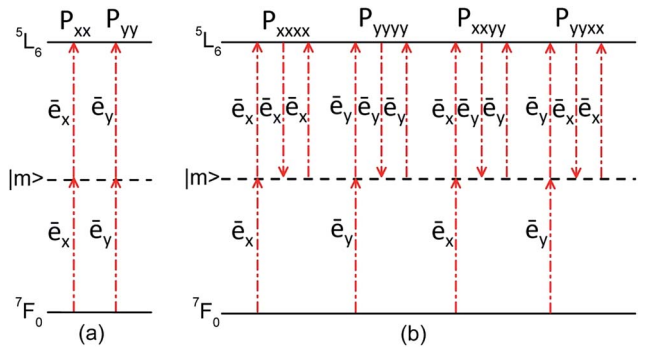

Fig. 6 The possible excitation pathways of non-resonant two-photon absorption and on-resonant four-photon absorption by the polarization modulated femtosecond laser field.

probability S_f in the excited state $^6P_{3/2}$ under the polarization modulated femtosecond laser field can be written as

$$S_f = \int_{-\infty}^{\infty} A_{abs}(\omega_f)\left(|P_{xx} + P_{xxxx}|^2 + |P_{yy} + P_{yyyy}|^2 + |P_{yyxx}|^2 + |P_{xxyy}|^2\right)d\omega_f. \quad (14)$$

It can be seen from eqn (14) that the total transition probability S_f is the interference result of the two-photon and four-photon absorption processes (*i.e.*, the two terms $|P_{xx} + P_{xxxx}|^2$ and $|P_{yy} + P_{yyyy}|^2$). For the transform-limited femtosecond laser field (*i.e.*, $\phi(\omega) = 0$), the two-photon transition amplitude $A_f^{(2)}$ is imaginary number (see eqn (1)), while four-photon transition amplitude $A_f^{(4)}$ is complex number, where the on-resonant part $A_f^{(4)on\text{-}res}$ is real number (see eqn (4)), while the near-resonant part $A_f^{(4)near\text{-}res}$ is imaginary number (see eqn (5)). It is evident that the two-photon absorption $A_f^{(2)}$ and the near-resonant four-photon absorption $A_f^{(4)near\text{-}res}$ can occur the destructive or constructive interference. Moreover, δ is the laser detuning (see eqn (5)), which will affect the sign of the near-resonant four-photon part $A_f^{(4)near\text{-}res}$ that depends on the laser central frequency, and finally determines the destructive or constructive interference of the two-photon and four-photon absorptions. In order to individually observe the contributions of the two-photon and four-photon absorptions in the whole excitation process, the transition probabilities of the excited state $^6P_{3/2}$ by the two-photon and four-photon absorptions are respectively given by

$$S_f^{(2)} = \int_{-\infty}^{\infty} A_{abs}(\omega_f)\left(|P_{xx}|^2 + |P_{yy}|^2\right)d\omega_f, \quad (15)$$

and

$$S_f^{(4)} = \int_{-\infty}^{\infty} A_{abs}(\omega_f)\left(|P_{xxxx}|^2 + |P_{yyyy}|^2 + |P_{yyxx}|^2 + |P_{xxyy}|^2\right)d\omega_f. \quad (16)$$

One can see from eqn (15) and (16) that the two-photon transition probability $S_f^{(2)}$ and four-photon transition probability $S_f^{(4)}$ are both dependent on the $\lambda/4$ wave plate rotation angle θ (*i.e.*, the laser polarization). It is easy to verify that both $S_f^{(2)}$ and $S_f^{(4)}$ are maximal value for $\theta = m\pi/2$ ($m = 0, 1, 2, \ldots$) and minimal value for $\theta = (2m + 1)\pi/4$, while their control efficiencies are different.

In order to explain the experimental observation that the polarization control efficiency of the up-conversion luminescence in Sm^{3+}-doped glass sample will decrease with the increase of the femtosecond laser intensity, as shown in Fig. 3. We theoretically calculate the normalized transition probability S_f by varying the quarter-wave plate angle θ based on eqn (14), together with the normalized two-photon and four-photon absorption contributions based on eqn (15) and (16) (*i.e.*, $S_f^{(2)}$ and $S_f^{(4)}$), and the simulated results are shown in Fig. 7. Here, these used parameters are mainly based on our experimental conditions, involving the laser wavelength, spectral bandwidth, laser intensity, state transition frequency of Sm^{3+} ions and state absorption bandwidth. As can be seen, both the two-photon and four-photon absorptions can be suppressed, and the maximal suppression occurs the same quarter-wave plate angle $\theta = (2m + 1)\pi/4$, but their control efficiency are different, and the four-photon absorption obtains the higher polarization control efficiency, which is consistent with above analysis. Furthermore, one can see from eqn (1) and (3)–(5) that the second-order term $A_f^{(2)}$ is proportional to $|E_0|^2$, while the fourth-order term $A_f^{(4)}$ is proportional to $|E_0|^4$, and therefore the relative weight of the four-photon absorption contribution in the whole excitation process will increase with the increase of the femtosecond laser intensity. As shown in eqn (14), the two-photon and four-photon absorption processes can generate the destructive or constructive interference. In our theoretical calculation, the interference between the two-photon and four-photon absorptions is destructive, and therefore the polarization control efficiency of the transition probability S_f will be suppressed (see Fig. 7), but the suppression degree depends on the weight of the four-photon absorption contribution in the whole excitation process. Thus, the experimental observation in Fig. 3 can be explained as follows. In the lower femtosecond laser intensity, the up-conversion luminescence mainly comes from the contribution of the two-photon absorption, and the polarization control efficiency is decided by the two-photon absorption, which is relatively large. However, the four-photon absorption contribution can be compared with the two-photon absorption contribution in the higher femtosecond laser intensity, and thus the destructive interference between the two-photon and four-photon absorptions will result in the decrease of the polarization control efficiency. Therefore, with the increase of the femtosecond laser intensity, the polarization control efficiency will decrease. It is obvious that the theoretical calculations are in good agreement with the experimental measurements.

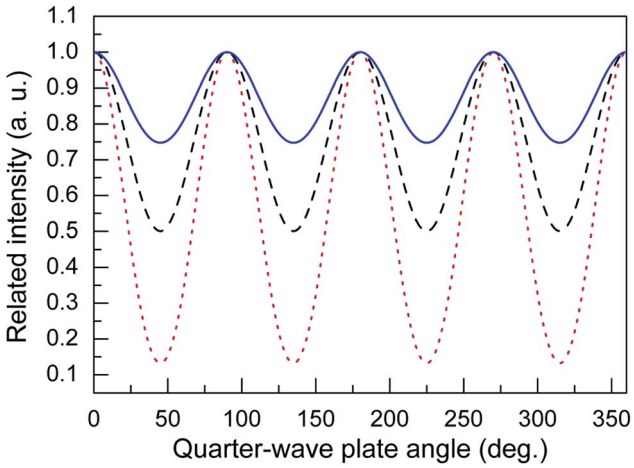

Fig. 7 The normalized excited state transition probability (blue solid line) under the intermediate femtosecond laser field by varying the quarter-wave plate angle θ, together with the normalized two-photon (black dashed line) and four-photon (red dotted line) absorption contributions.

4. Conclusions

In summary, we have experimentally demonstrated that, under the intermediate femtosecond laser field excitation, the polarization control efficiency of the up-conversion luminescence in the Sm^{3+}-doped glass will be affected by the laser intensity, and the experimental results showed that the polarization control efficiency of the up-conversion luminescence will decrease with the increase of the femtosecond laser intensity. We theoretically proposed a four-order perturbation theory (*i.e.*, the higher nonlinear optical effect) to explain the experimental observation by considering both the two-photon and four-photon absorption processes, and the theoretical calculations showed that the destructive interference between two- and four-photon excitation pathways results in the decrease of the polarization control efficiency because of their different polarization control efficiency degrees. In this work, we extend the polarization control behavior of the up-conversion luminescence in rare-earth ions to the intermediate femtosecond laser field, which is very useful for further understanding and controlling the up-conversion luminescence process under the intermediate femtosecond laser field. Furthermore, these theoretical and experimental studies are also expected to be applied in related application areas.

Acknowledgements

This work was partly supported by Program of Introducing Talents of Discipline to Universities (B12024), National Natural Science Foundation of China (No. 11474096), Science and Technology Commission of Shanghai Municipality (No. 14JC1401500 and No. 16520721200), and Higher Education Key Program of He'nan Province of China (No. 17A140025).

References

1 F. Auzel, Up-conversion and anti-stokes processes with f and d ions in solids, *Chem. Rev.*, 2004, **104**, 139–174.
2 F. Wang and X. Liu, Recent advances in the chemistry of lanthanide-doped upconversion nanocrystals, *Chem. Soc. Rev.*, 2009, **38**, 976–989.
3 R. Scheps, Up-conversion laser processes, *Prog. Quantum Electron.*, 1996, **20**, 271–358.
4 E. Wintner, E. Sorokin and I. T. Sorokina, Recent developments in diode-pumped ultrashort pulse solid-state lasers, *Laser Phys.*, 2001, **11**, 1193–1200.
5 N. Tessler, V. Medvedev, M. Kazes, S. H. Kan and U. Banin, Efficient near-infrared polymer nanocrystal light-emitting diodes, *Science*, 2002, **295**, 1506–1508.
6 P. Zhou, X. Wang, Y. Ma, H. Lü and Z. J. Liu, Review on recent progress on mid-infrared fiber lasers, *Laser Phys.*, 2012, **22**, 1744–1751.
7 S. Sivakumar, F. C. M. van Veggel and M. Raudsepp, Bright white light through up-conversion of a single NIR source from sol–gel-derived thin film made with Ln^{3+}-doped LaF_3 nanoparticles, *J. Am. Chem. Soc.*, 2005, **127**, 12464–12465.
8 H. Q. Wang, M. Batentschuk, A. Osvet, L. Pinna and C. J. Brabec, Rare-earth ion doped up-conversion materials for photovoltaic applications, *Adv. Mater.*, 2011, **23**, 2675–2680.
9 E. Downing, L. Hesselink, J. Ralston and R. Macfarlane, A three-color, solid-state, three-dimensional display, *Science*, 1996, **273**, 1185–1189.
10 Y. Li, J. Zhang, Y. Luo, X. Zhang, Z. Hao and X. Wang, Color control and white light generation of up-conversion luminescence by operating dopant concentrations and pump densities in Yb^{3+}, Er^{3+} and Tm^{3+} tri-doped Lu_2O_3 nanocrystals, *J. Mater. Chem.*, 2011, **21**, 2895–2900.
11 M. Nyk, R. Kumar, T. Y. Ohulchansky, E. J. Bergey and P. N. Prasad, High contrast *in vitro* and *in vivo* photoluminescence bio-imaging using near infrared to near infrared up-conversion in Tm^{3+} and Yb^{3+} doped fluoride nanophosphors, *Nano Lett.*, 2008, **8**, 3834–3838.
12 F. Wang, W. B. Tan, Y. Zhang, X. Fan and M. Wang, Luminescent nanomaterials for biological labelling, *Nanotechnology*, 2005, **17**, R1–R13.
13 M. Yu, F. Li, Z. Chen, H. Hu, C. Zhan, H. Yang and C. Huang, Laser scanning up-conversion luminescence microscopy for imaging cells labeled with rare-earth nanophosphors, *Anal. Chem.*, 2009, **81**, 930–935.
14 F. Vetrone, R. Naccache, A. Zamarrón, A. Juarranz de la Fuente, F. Sanz-Rodríguez, E. Martin Rodringuez, D. Jaque, J. Garcia Sole and J. A. Capobianco, Temperature sensing using fluorescent nanothermometers, *ACS Nano*, 2010, **4**, 3254–3258.
15 X. Tian, Z. Wu, Y. Jia, J. Chen, R. K. Zheng, Y. Zhang and H. Lu, Remanent-polarization-induced enhancement of photoluminescence in Pr^{3+}-doped lead-free ferroelectric $(Bi_{0.5}Na_{0.5})TiO_3$ ceramic, *Appl. Phys. Lett.*, 2013, **102**, 042907.
16 V. K. Tikhomirov, L. F. Chibotaru, D. Saurel, P. Gredin, M. Mortier and V. V. Moshchalkov, Er^{3+}-doped nanoparticles for optical detection of magnetic field, *Nano Lett.*, 2009, **9**, 721–724.
17 S. Schietinger, T. Aichele, H. Q. Wang, T. Nann and O. Benson, Plasmon-enhanced up-conversion in single $NaYF^4$:Yb^{3+}/Er^{3+} co-doped nanocrystals, *Nano Lett.*, 2009, **10**, 134–138.
18 C. D. Brites, P. P. Lima, N. J. Silva, A. Millán, V. S. Amaral, F. Palacio and L. D. Carlos, A luminescent molecular thermometer for long-term absolute temperature measurements at the nanoscale, *Adv. Mater.*, 2010, **22**, 4499–4504.
19 J. Zhou, J. Deng, H. Zhu, X. Chen, Y. Teng, H. Jia, S. Q. Xu and J. R. Qiu, Up-conversion luminescence in LaF^3:Ho^{3+} *via* two-wavelength excitation for use in solar cells, *J. Mater. Chem. C*, 2013, **1**, 8023–8027.
20 R. Deng, F. Qin, R. Chen, W. Huang, M. Hong and X. Liu, Temporal full-colour tuning through non-steady-state up-conversion, *Nat. Nanotechnol.*, 2015, **10**, 237–242.
21 C. F. Gainer, G. S. Joshua, C. R. De Silva and M. Romanowski, Control of green and red up-conversion in $NaYF^4$:Yb^{3+}, Er^{3+} nanoparticles by excitation modulation, *J. Mater. Chem.*, 2011, **21**, 18530–18533.

22 S. Zhang, S. Xu, J. Ding, C. Lu, T. Jia, J. Qiu and Z. Sun, Single and two-photon fluorescence control of Er^{3+} ions by phase-shaped femtosecond laser pulse, *Appl. Phys. Lett.*, 2014, **104**, 014101.
23 S. Zhang, C. Lu, T. Jia, J. Qiu and Z. Sun, Coherent phase control of resonance-mediated two-photon absorption in rare-earth ions, *Appl. Phys. Lett.*, 2013, **103**, 194104.
24 Y. Yao, S. Zhang, H. Zhang, J. Ding, T. Jia, J. Qiu and Z. Sun, Laser polarization and phase control of up-conversion fluorescence in rare-earth ions, *Sci. Rep.*, 2014, **4**, 7295.
25 H. Zhang, Y. Yao, S. Zhang, C. Lu and Z. Sun, Up-conversion luminescence polarization control in Er^{3+}-doped $NaYF_4$ nanocrystals, *Chin. Phys. B*, 2015, **25**, 23201.
26 D. Meshulach and Y. Silberberg, Coherent quantum control of multiphoton transitions by shaped ultrashort optical pulses, *Phys. Rev. A*, 1999, **60**, 1287–1292.
27 L. Chuntonov, L. Rybak, A. Gandman and Z. Amitay, Frequency-domain coherent control of femtosecond two-photon absorption: intermediate-field *versus* weak-field regime, *J. Phys. B: At., Mol. Opt. Phys.*, 2008, **41**, 035504.
28 L. Chuntonov, L. Rybak, A. Gandman and Z. Amitay, Enhancement of intermediate-field two-photon absorption by rationally shaped femtosecond pulses, *Phys. Rev. A*, 2008, **77**, 021403.
29 L. Chuntonov, L. Rybak, A. Gandman and Z. Amitay, Intermediate-field two-photon absorption enhancement by shaped femtosecond pulses: tolerance to phase deviation from perfect antisymmetry, *Phys. Rev. A*, 2010, **81**, 045401.
30 S. Xu, Y. Huang, Y. Yao, T. Jia, J. Ding, S. Zhang and Z. Sun, Polarization control of intermediate state absorption in resonance-mediated multi-photon absorption process, *J. Phys. B: At., Mol. Opt. Phys.*, 2015, **48**, 135402.